Electronic Supplementary Information for:

Magnetic Frustration in a Hexaazatrinaphthylene-Bridged Trimetallic Dysprosium Single-Molecule Magnet

General Synthetic Details. All manipulations were carried out under dry, oxygen-free argon using standard Schlenk-line and glove-box techniques. Toluene was dried by refluxing over potassium for at least 3 days prior to distillation. The solvent was then transferred onto 4 Å molecular sieves and degassed with three freeze-pump-thaw cycles. Dysprosium nitrate hydrate and 2,2,6,6-tetramethylheptanedione (Hthd) were purchased from Alfa Aesar and Sigma Aldrich, respectively, and used as received. Tris(2,2,6,6-tetramethylheptanedionato)dysprosium(III) and hexaazatrinapthalene were prepared according to literature procedures.[1,2] Elemental analysis was carried out at London Metropolitan University, UK. IR spectroscopy was carried out on a solid sample using a Bruker Alpha Diamond ATR spectrometer. UV-vis-NIR spectroscopy was carried out on a PerkinElmer Lambda-1050 spectrometer in the range $\lambda = 300\text{-}1600$ nm. X-Ray diffraction data was obtained using an Oxford Instruments XCalibur2 diffractometer using MoKα radiation.

Synthesis of [{(thd)$_3$Dy}$_3$HAN]·3(toluene) [1·3(toluene)]. Toluene (10 mL) was added to a mixture of Dy(thd)$_3$ (1.00 g, 1.40 mmol) and HAN (0.18 g, 0.47 mmol) at room temperature. The solution immediately turned dark red, with a small amount of yellow solid remaining, and the reaction was stirred at room temperature for 40 minutes until all of the yellow solid had been consumed. The mixture was filtered and concentrated to approximately 5 mL. The resulting precipitate was re-dissolved with gentle heating. Dark red crystals formed overnight upon storage at 2.5°C. A second crop of crystals was isolated after concentrating the supernatant solution (total isolated yield: 1.01 g, 86 %). Elemental analysis (%): calculated, C 58.59, H 7.31, N 3.33; found, C 58.66, H 7.45, N 3.22.

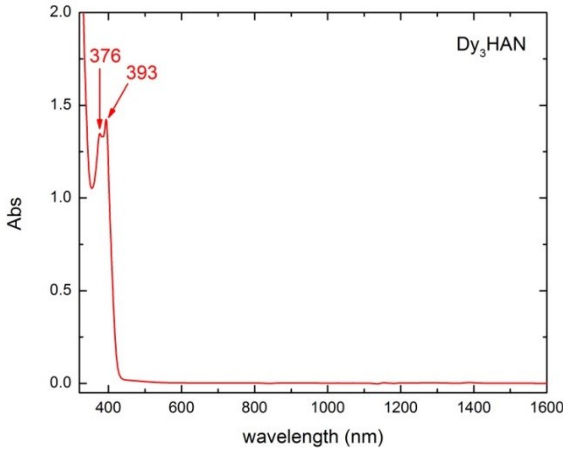

Figure S1. UV-vis spectrum of **1**·3(toluene) in toluene.

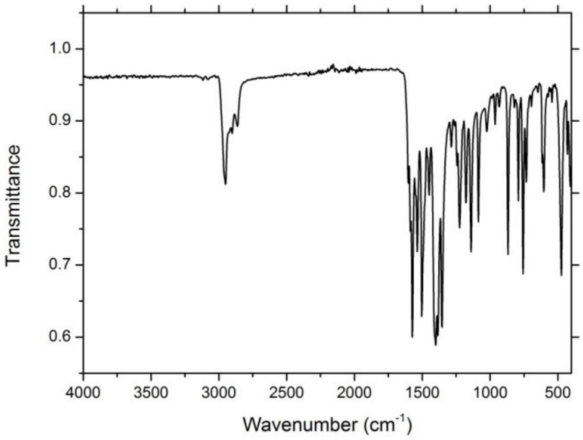

Figure S2. IR spectrum of solid sample of **1**·3(toluene).

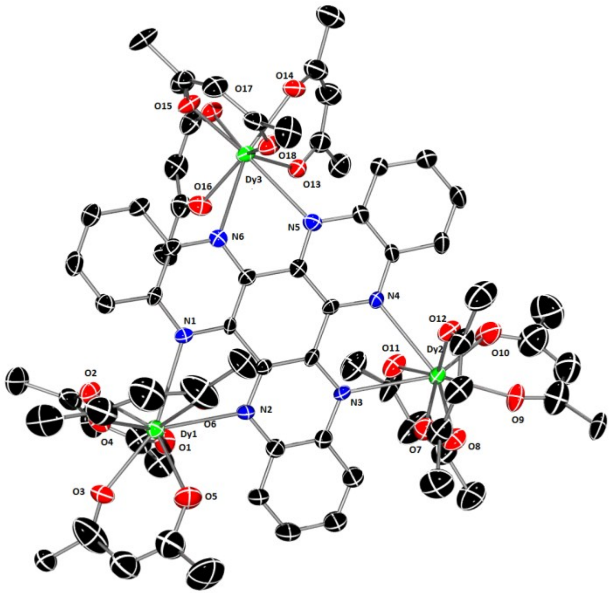

Figure S3. ORTEP structure of **1** with thermal ellipsoids set at 50% probability level. Dy = green, O = red, N = blue, C = black (hydrogen atoms and CH_3 groups omitted for clarity).

Table S1. Crystal data and structure refinement for **1**·3(toluene).

Empirical formula	$C_{144}H_{207}Dy_3N_6O_{18}$
Formula weight	2797.64
Temperature/K	100
Crystal system	monoclinic
Space group	$P2_1/c$
a/Å	30.2821(16)
b/Å	13.7793(5)
c/Å	34.9863(9)
α/°	90
β/°	96.055(3)
γ/°	90
Volume/Å^3	14517.1(10)
Z	4
ρ_{calc}g/cm^3	1.280
μ/mm^{-1}	1.590
F(000)	5820.0
Crystal size/mm^3	0.1 × 0.1 × 0.05
Radiation	MoKα (λ = 0.71073)
2Θ range for data collection/°	5.944 to 50.7
Reflections collected	54065
Independent reflections	26550
Data/restraints/parameters	26550/883/1699
Goodness-of-fit on F^2	1.075
Final R indexes [I>=2σ (I)]	$R_1 = 0.0633$, $wR_2 = 0.1408$
Largest diff. peak/hole / e Å^{-3}	1.64/-1.02
CCDC ref. code	1478313

Table S2. Selected bond lengths (Å) for **1**.

Bond	Length
Dy1–O1	2.297(5)
Dy1–O2	2.307(5)
Dy1–O3	2.298(5)
Dy1–O4	2.256(5)
Dy1–O5	2.268(6)
Dy1–O6	2.342(5)
Dy1–N1	2.669(5)
Dy1–N2	2.646(6)
Dy2–O7	2.292(5)
Dy2–O8	2.271(5)
Dy2–O9	2.315(6)
Dy2–O10	2.251(6)
Dy2–O11	2.300(6)
Dy2–O12	2.285(5)
Dy2–N3	2.694(6)
Dy2–N4	2.699(6)
Dy3–O13	2.308(5)
Dy3–O14	2.259(5)
Dy3–O15	2.291(5)
Dy3–O16	2.263(5)
Dy3–O17	2.318(5)
Dy3–O18	2.305(5)
Dy3–N5	2.696(6)
Dy3–N6	2.760(6)

Magnetic property measurements

The magnetic properties of **1**·3(toluene) were measured on a Quantum Design MPMS-7 SQUID magnetometer in a temperature range 1.8-300 K. The sample was prepared by restraining a polycrystalline sample in eicosane and flame-sealed in an NMR tube under vacuum.

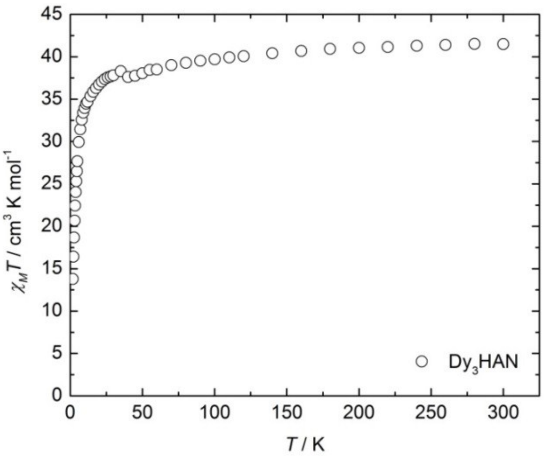

Figure S4. The product of the molar magnetic susceptibility with temperature (χ_MT) against temperature (T) for **1**·3(toluene).

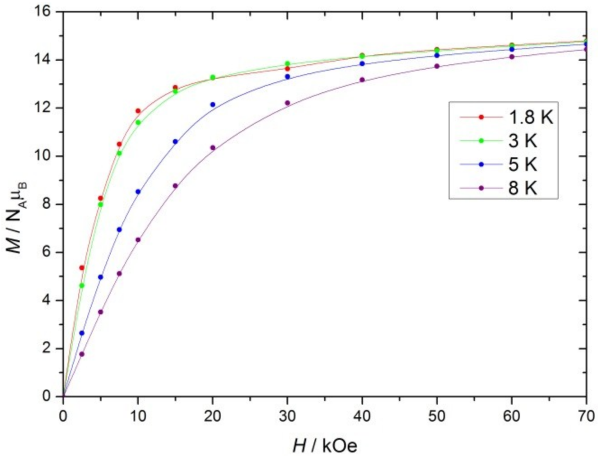

Figure S5. Field dependence of the magnetization for **1**·3(toluene). The solid lines are a guide for the eye.

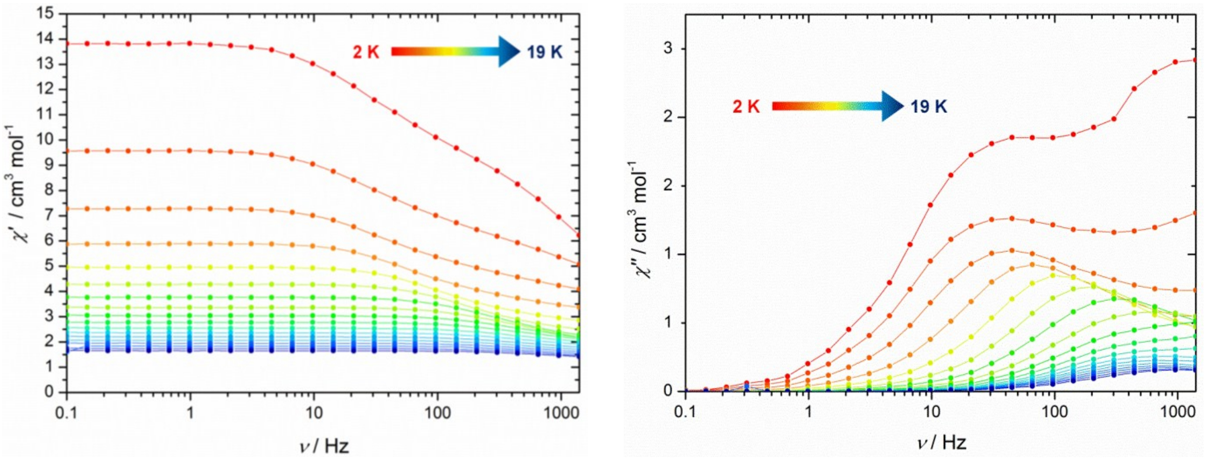

Figure S6. Frequency dependence of the in-phase (χ') and the out-of-phase (χ'') magnetic susceptibility for **1**·3(toluene) using an oscillating field of H_{ac} = 1.55 Oe and zero applied field.

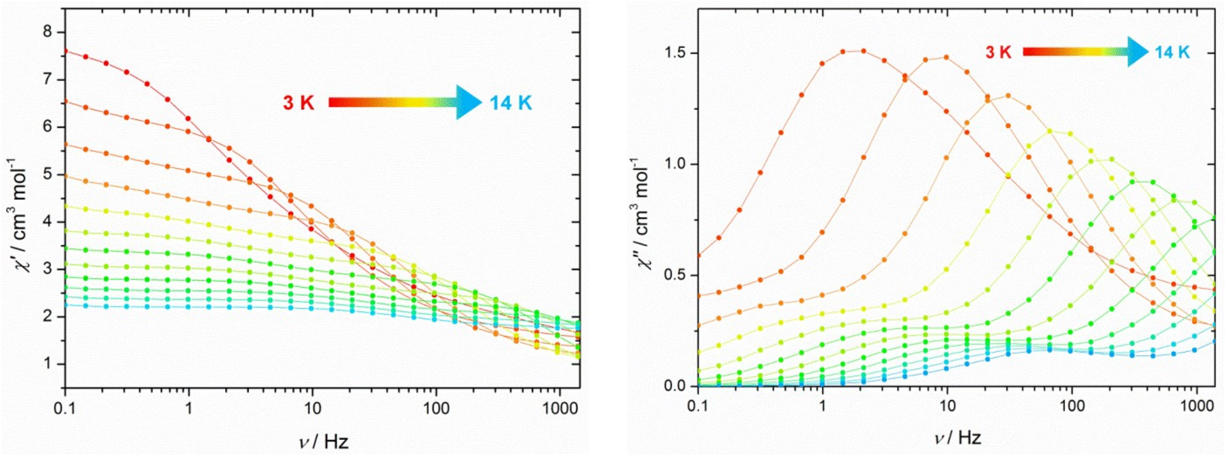

Figure S7. Frequency dependence of the in-phase (χ') and the out-of-phase (χ'') magnetic susceptibility for **1**·3(toluene) using an oscillating field of H_{ac} = 1.55 Oe and an applied field of H_{dc} = 1 kOe.

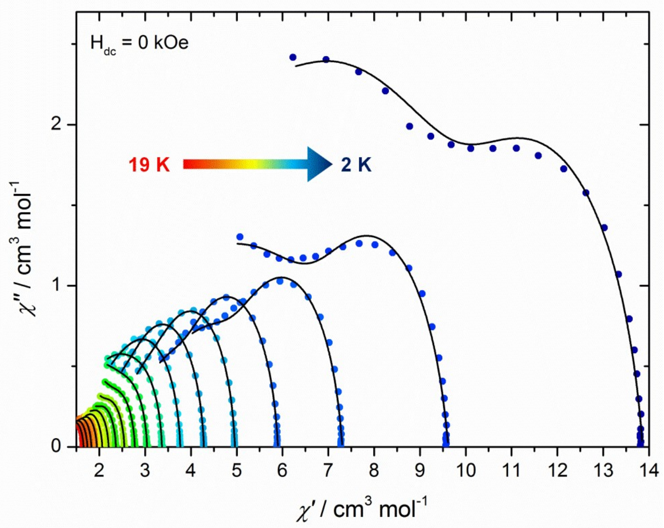

Figure S8. Argand diagram for **1**·3(toluene) in zero d.c. field.

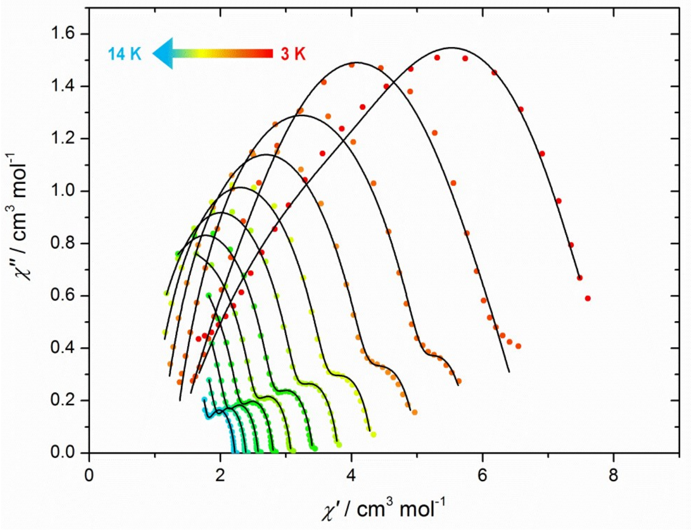

Figure S9. Argand diagram for **1**·3(toluene) in an applied field of H_{dc} = 1 kOe.

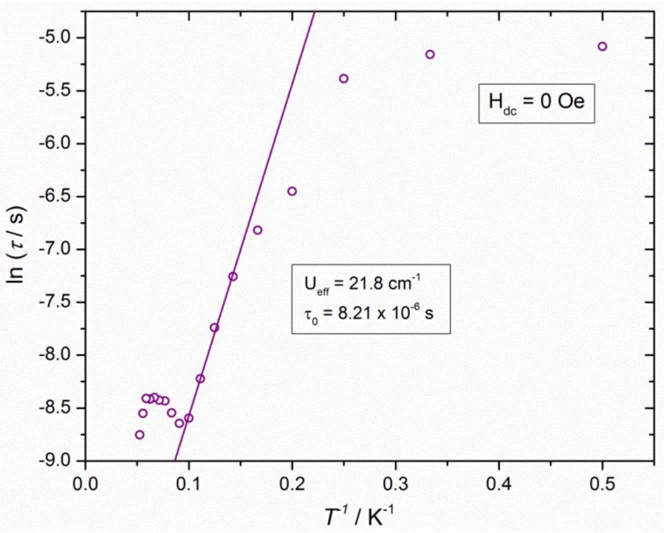

Figure S10. Arrhenius plots of ln τ vs. T^{-1} for **1**·3(toluene) in zero d.c. field.

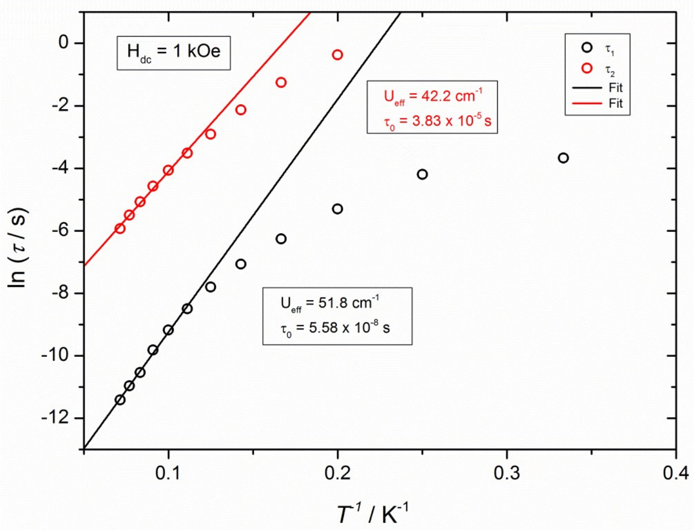

Figure S11. Arrhenius plots of ln τ vs. T^{-1} for **1**·3(toluene) in an applied field of H_{dc} = 1 kOe.

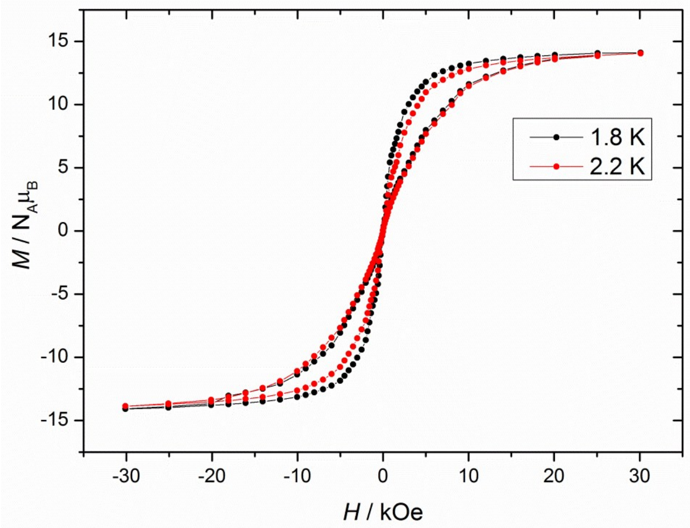

Figure S12. Magnetization (M) vs. field (H) hysteresis loops for **1**·3(toluene) at 1.8 K and 2.2 K, using an average sweep rate of 1.93 mT s^{-1}.

Computational details

All calculations were carried out with MOLCAS 8.0 and are of the CASSCF/RASSI/SINGLE_ANISO type. The Cholesky decomposition threshold was set to $5 \cdot 10^{-9}$ to save disk space. Each Dy centre was calculated by using the fragment shown in Figure S13.

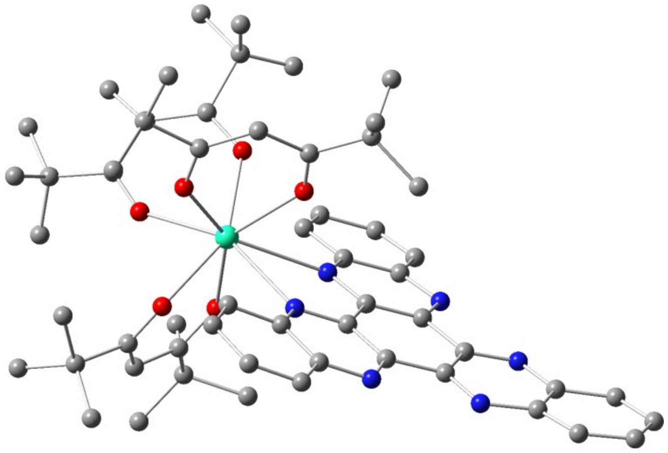

Figure S13. Structure of the calculated $[(\mathrm{thd})_3\mathrm{Dy(HAN)}]$ fragments. The hydrogen atoms are not shown.

Two basis set approximations have been employed: Basis 1 – small, and Basis 2 – large. Table S3 shows the contractions of the employed basis sets for all elements.

Table S3. Contractions of the employed basis sets in computational approximations **1** and **2**.

Basis 1	**Basis 2**
Dy.ANO-RCC-VDZP.	Dy.ANO-RCC-VTZP
O.ANO-RCC-VDZ	O.ANO-RCC-VDZP
N.ANO-RCC-VDZ	N.ANO-RCC-VDZP (close)
C.ANO-RCC-VDZ	N.ANO-RCC-VDZ (distant)
H.ANO-RCC-VDZ	C.ANO-RCC-VDZ
	H.ANO-RCC-VDZ

The active space of the CASSCF method included 9 electrons in 7 orbitals (4*f* orbitals of Dy^{3+} ion). We have mixed 21 sextets, 128 quartet and 130 doublet states by spin-orbit coupling. On the basis of the resulting spin-orbital multiplets, the SINGLE_ANISO program computed the local magnetic properties (*g*-tensors, magnetic axes, local magnetic susceptibility, etc.).

Table S4. Energies of the lowest Kramers doublets (cm^{-1}) of the Dy centres in complex **1**.

Spin-orbit energies, cm^{-1}					
Dy1_basis1	**Dy1_basis2**	**Dy2_basis1**	**Dy2_basis2**	**Dy3_basis1**	**Dy3_basis2**
0	0	0	0	0	0
91	121	107	152	38	64
188	238	177	252	135	177
239	314	249	336	230	279
304	379	333	421	310	369
371	446	412	505	401	470
422	549	501	627	456	542
641	710	665	794	556	621

Table S5. The *g*-factors of the lowest Kramers doublets (KD) of Dy centres in complex **1**.

KD		**Dy1_basis1**	**Dy1_basis2**	**Dy2_basis1**	**Dy2_basis2**	**Dy3_basis1**	**Dy3_basis2**
		g	***g***	***g***	***g***	***g***	***g***
1	g_X	0.031	0.016	0.0071	0.0019	0.0046	0.0093
	g_Y	0.067	0.030	0.016	0.0046	0.039	0.018
	g_Z	19.05	19.29	19.69	19.95	19.03	19.12
2	g_X	0.18	0.098	0.054	0.0027	0.044	0.024
	g_Y	0.22	0.11	0.056	0.011	0.12	0.038
	g_Z	16.46	16.53	16.52	16.69	16.71	16.75
3	g_X	0.37	0.13	0.34	0.18	0.27	0.079
	g_Y	0.74	0.31	0.41	0.28	0.37	0.15
	g_Z	14.65	14.38	14.48	14.31	13.67	13.84
4	g_X	1.89	0.48	0.54	1.35	0.95	1.13
	g_Y	3.49	1.00	1.31	2.03	1.45	1.28
	g_Z	11.80	11.89	11.05	11.36	11.01	10.98

Account of the total magnetic interactions

Only one exchange fitting parameter was used for all Dy-Dy interactions, by using the following Hamiltonian:

$$\hat{H} = -[(J_{12}^{dip} + J^{exch})\hat{\tilde{s}}_{1,z1}\hat{\tilde{s}}_{2,z2} + (J_{13}^{dip} + J^{exch})\hat{\tilde{s}}_{1,z1}\hat{\tilde{s}}_{3,z3} + (J_{23}^{dip} + J^{exch})\hat{\tilde{s}}_{2,z2}\hat{\tilde{s}}_{3,z3}]$$

The Ising exchange parameters were calculated from Lines parameters by the expression:

$$J_{ij}^{Ising} = 25 J_{Lines} \cos\varphi_{ij}$$

where φ_{ij} is the angle between the main anisotropy axes of the interacting sites.

The Lines parameter has been determined by fitting the experimental magnetic susceptibility data (Figure S14). The dipolar parameters were calculated straightforwardly.

Table S6. Exchange interactions between Dy ions in complex **1**. Ising parameters (cm^{-1}).

Molecule/approximation		$\mathbf{J_{dip}}^*$	$\mathbf{J_{exch}}$
Basis2	Dy1-Dy2	-0.29	-2.3
	Dy1-Dy3	-0.29	-2.3
	Dy2-Dy3	-0.28	-2.5

*contribution only from the Ising terms $\sim \hat{\tilde{s}}_{1,z}\hat{\tilde{s}}_{2,z}$ to the dipolar coupling. In the calculation of the exchange spectrum the dipolar interaction included all terms.

Table S7. Energies (cm^{-1}) of the lowest exchange states in **1**, considering the total magnetic interaction.

Basis 2
0.00000
0.00000
0.00175
0.00175
0.08040
0.08040
2.47372
2.47372

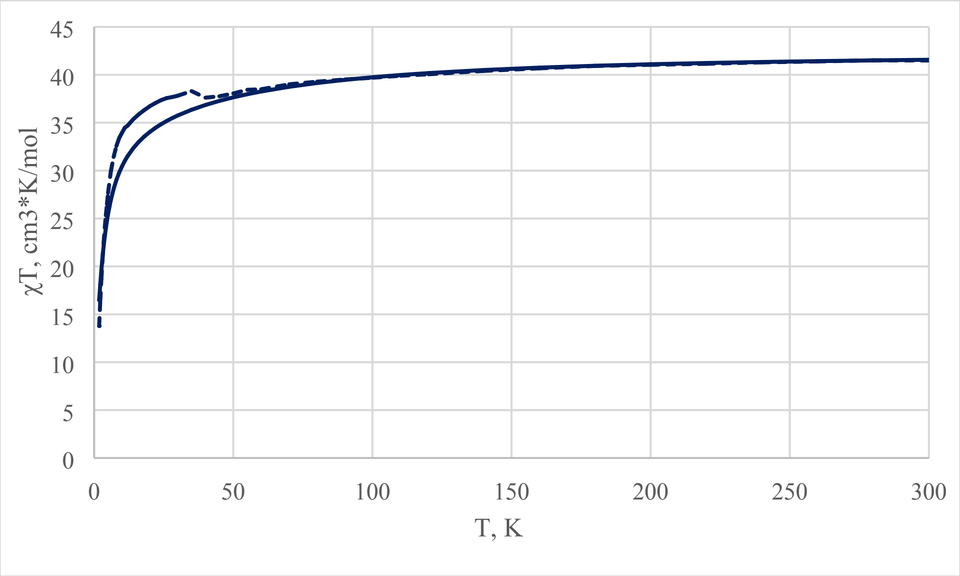

Figure S14. Experimental *vs*. calculated magnetic susceptibility for **1**. zJ'=-0.01 cm^{-1}.

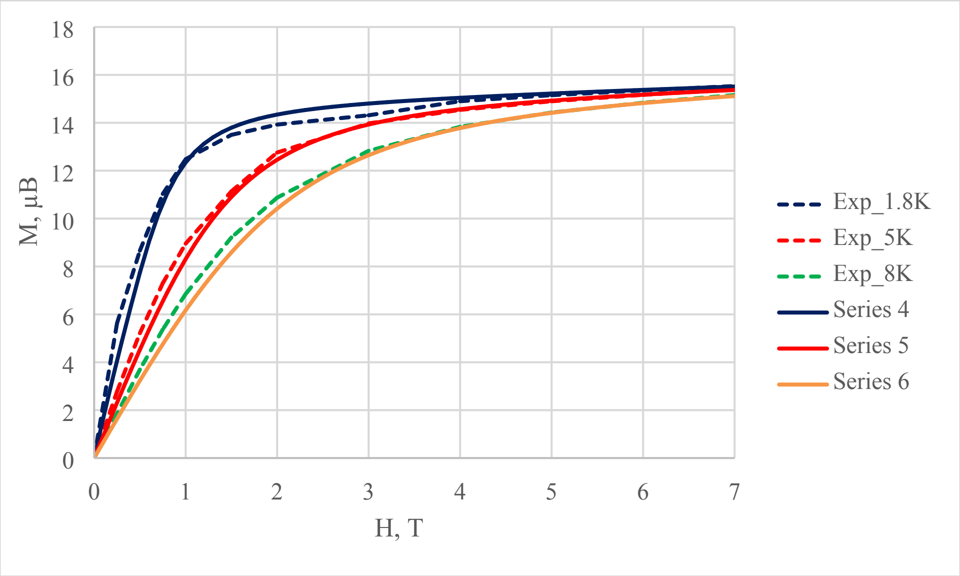

Figure S15. Experimental *vs*. calculated magnetization for **1**. zJ'=-0.01 cm^{-1}.

References

1. K. J. Eisentraut, R. E. Sievers, D. Coucouvanis and J. P. Fackler, *Inorg. Synth*., 2007, **11**, 94.
2. S. Barlow, Q. Zhang, B. R. Kaafarani, C. Risko, F. Amy, C. K. Chan, B. Domercq, Z. A. Starikova, M. Y. Antipin, T. V. Timofeeva, B. Kippelen, J-L. Brédas, A. Kahn and S. R. Marder, *Chem. Eur. J.,* 2007, **13**, 3537.